JMEPEG (2011) 20:1631–1637
DOI: 10.1007/s11665-011-9839-x

1059-9495/$19.00

Galvanic Corrosion of a Carbon Steel-Stainless Steel Couple in Sulfide Solutions

C.F. Dong, K. Xiao, X.G. Li, and Y.F. Cheng

(Submitted May 20, 2010; in revised form January 3, 2011)

The galvanic corrosion behavior of carbon steel-stainless steel couples with various cathode/anode area ratios was investigated in S^{2-}-containing solutions, which were in equilibrium with air, by electrochemical measurements, immersion test, and surface characterization. It is found that the galvanic corrosion effect on carbon steel anode increases with the cathode/anode area ratios, and decreases with the increasing concentration of S^{2-} in the solution. A layer of sulfide film is formed on carbon steel surface, which protects it from corrosion. When the cathode/anode area ratio is 1:1, the potentiodynamic polarization curve measurement and the weight-loss determination give the identical measurement of the galvanic corrosion effect. With the increase of the cathode/anode area ratio, the electrochemical method may not be accurate to determine the galvanic effect. The anodic dissolution current density of carbon steel cannot be approximated simply with the galvanic current density.

Keywords carbon steel, galvanic corrosion, stainless steel

1. Introduction

Duplex systems with a carbon steel core and a stainless steel outer-housing have been widely used in petrochemical industry to take advantage of the low cost of carbon steel and a high corrosion resistance provided by stainless steel (Ref 1). However, the accelerated corrosion of the more active metal, i.e., carbon steel, due to electrical coupling to the more noble metal, i.e., stainless steel, in a corrosive environment, which is so called galvanic corrosion, has been one of the most primary problems that shorten the service life span of the duplex system. Galvanic corrosion behavior between two dissimilar metals has been investigated extensively, and key parameters affecting the corrosion of the active metal has been determined. For example, Mansfeld (Ref 2) derived equations to calculate galvanic potential and galvanic current for a series of galvanic couples. Akid and Mills (Ref 3) introduced a scanning reference electrode technique (SRET) in galvanic corrosion research, and characterized the potential distribution of a galvanic couple. Furthermore, it has been accepted (Ref 4-10) that the galvanic corrosion behavior is influenced not only by the electrochemical properties of the target metals, but also by various environmental parameters, including solution conductivity and pH, cathode/anode area ratio, distance between the two metals in the couple, temperature, solution flow speed, etc.

C.F. Dong, K. Xiao, and **X.G. Li**, Corrosion and Protection Center, University of Science and Technology Beijing, Beijing 100083, China; Key Laboratory of Corrosion and Protection, Chinese Ministry of Education, Beijing 100083, China; and **Y.F. Cheng**, Department of Mechanical & Manufacturing Engineering, University of Calgary, Calgary, AB T2N 1N4, Canada. Contact e-mails: cfdong@ustb.edu.cn and fcheng@ucalgary.ca.

Galvanic corrosion occurring in petrochemical environments that contain sulfide is an essential problem affecting the safety and operation of facilities (Ref 11, 12). In this study, the galvanic corrosion behavior of a carbon steel-stainless steel couple in sulfide solutions was investigated by potentiodynamic polarization curve and zero-resistance ammeter (ZRA) measurements, immersion test, and scanning electron microscopy (SEM) and energy-dispersive x-ray (EDX) characterization. The parametric effects, such as sulfide concentration and cathode/anode area ratio, on galvanic corrosion were determined. The galvanic corrosion behavior of carbon steel was analyzed quantitatively.

2. Experimental

The materials used in this study included a 304 L stainless steel and a 1020 carbon steel, with chemical compositions (wt.%) shown in Table 1. The two steel samples were directly contacted together, and sealed with a LECO epoxy. With other faces sealed in the epoxy, the working face of the galvanic couple was ground sequentially to 1200 grit emery paper, cleaned in distilled water, dried, and kept for test.

The test solutions contained 0.1 M NaCl and Na_2S with various concentrations. All solutions were made from analytic grade chemicals, and were in equilibrium with air. The solution pH varied from 12 to 13.5, depending on the sulfide concentration contained in the solution. All tests were conducted at 25 ± 0.5 °C controlled in a water bath.

The potentiodynamic polarization curves were measured using a PAR 273 potentiostat (EG&G) on a three-electrode cell, where the steel electrode was used as working electrode (WE), a saturated calomel electrode (SCE) as reference electrode and a platinum plate as auxiliary electrode. The potential scanning rate was 1 mV/s, with the potential scanning range from −500 mV versus corrosion potential (E_{corr}) to 700 mV versus E_{corr}.

Table 1 Chemical compositions of the tested steels in a galvanic couple (wt.%)

Steels	C	Si	Mn	P	S	Cr	Ni	Fe
1020 carbon steel	0.10	0.20	0.37	0.019	0.012	…	…	Balance
304 L stainless steel	0.03	0.52	1.03	0.017	0.006	18.01	9.60	Balance

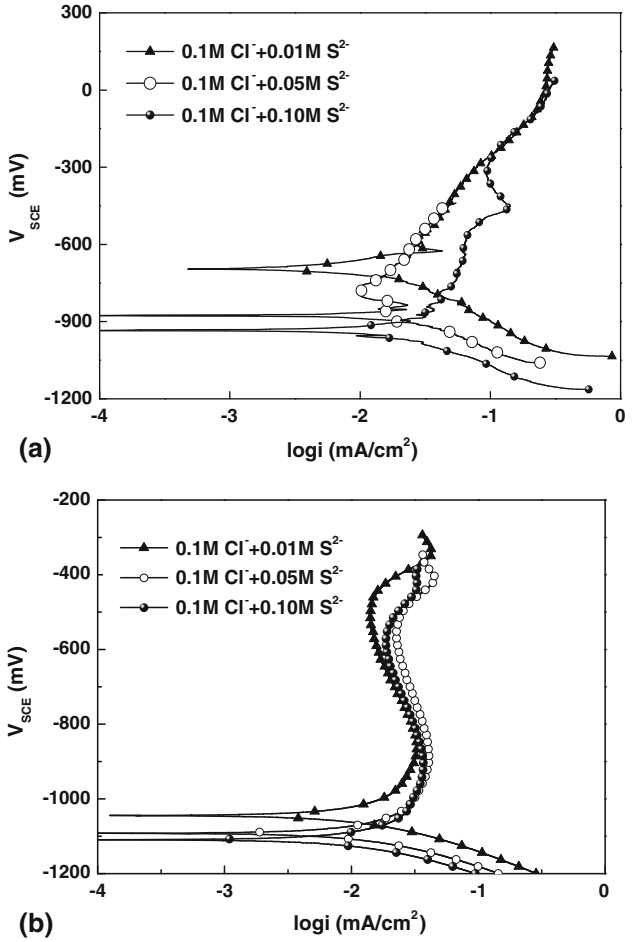

Fig. 1 Potentiodynamic polarization curves of (a) 1020 carbon steel and (b) 304 L stainless steel in 0.1 M NaCl + Na_2S solutions with different S^{2-} concentrations

Table 2 Corrosion potential and corrosion current density of 1020 carbon steel and 304 L stainless steel in test solutions with various concentrations of S^{2-}

Solutions	Materials	E_{corr}, mV, SCE	i_{corr}, μA/cm²
0.1 M NaCl + 0.01 M Na_2S	304 L	−530	0.67
	1020	−696	1.48
0.1 M NaCl + 0.05 M Na_2S	304 L	−691	0.64
	1020	−877	1.45
0.1 M NaCl + 0.10 M Na_2S	304 L	−695	0.58
	1020	−935	1.55

A zero-resistance ammeter (ZRA) was used to connect the 304 L stainless steel and 1020 carbon steel electrodes, which were employed as WE1 and WE2, respectively. The specimens were mounted in epoxy resin, and the surface area of the carbon steel electrode, i.e., WE2, was fixed at 1 cm^2. The area of the stainless steel electrode, i.e., WE1, was changed to generate the ratios of the surface area of WE1 to WE2 to be 1:1, 2:1 and 10:1, respectively. Prior to test, the electrodes were immersed in the test solution for 20 min. Measurements were then conducted to record galvanic potential, E_g, and galvanic current, I_g. The immersion times were 5, 10, and 15 days, and simultaneously, the change of the solution pH was measured. After test, the electrodes were removed and rinsed in distilled water

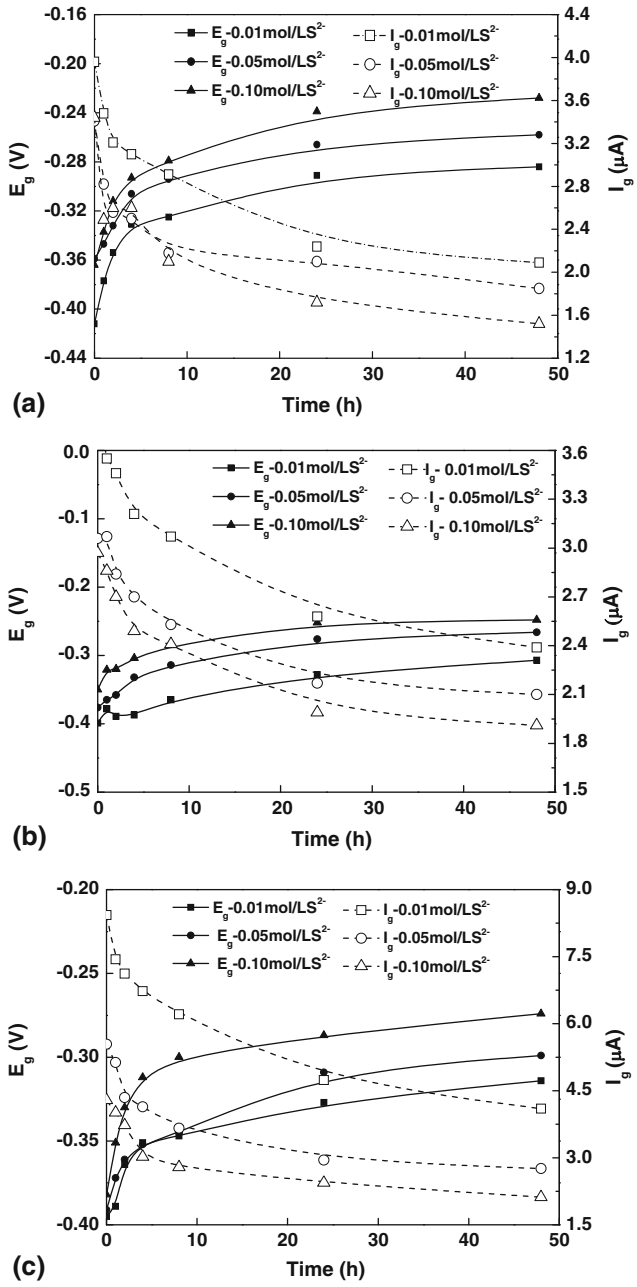

Fig. 2 Galvanic potential (E_g) and galvanic current (I_g) measured under various cathode/anode area ratios and the concentration of S^{2-}: (a) S_c:S_a = 1:1, (b) S_c:S_a = 2:1, (c) S_c:S_a = 10:1

and acetone, and dried to determine the weight-loss. The corrosion product on the electrode surface was carefully removed with a descaling solution (100 mL H_3PO_4 + 20 g CrO_3 + 900 mL H_2O, 90 °C).

Furthermore, the surface of the specimen was characterized by a Model LEO-1450 SEM. The surface corrosion product was analyzed by an EDX detector combined with SEM.

3. Results

3.1 Potentiodynamic Polarization Measurements

Figure 1 shows the potentiodynamic polarization curves measured on carbon steel (a) and stainless steel (b) electrodes in solutions containing various concentrations of S^{2-}. It is shown that corrosion potential of the carbon steel electrode decreased with the increasing S^{2-} concentration in the solution, while that of the stainless steel electrode did not show an apparent change. The electrochemical parameters were obtained by fitting the measured polarization curves with the EG&G software provided, and the results are shown in Table 2. It is realized that the fitting of the electrochemical parameters exists some uncertainties. Thus, the parameters obtained are primarily used for a qualitative comparison. It is seen that, at individual solution, there was a more negative E_{corr} and a higher corrosion current density of carbon steel than those of stainless steel. Moreover, with the increase of the S^{2-} concentration, the corrosion current density for both electrodes decreased.

3.2 ZRA Measurements

Figure 2 shows the galvanic potential and galvanic current measured on the stainless steel-carbon steel couple with various cathode/anode area ratios in the test solutions containing various concentrations of S^{2-}. It is seen that both galvanic potential and galvanic current approached relatively stable values with time. At individual cathode/anode area ratio, galvanic potential increased, while galvanic current decreased

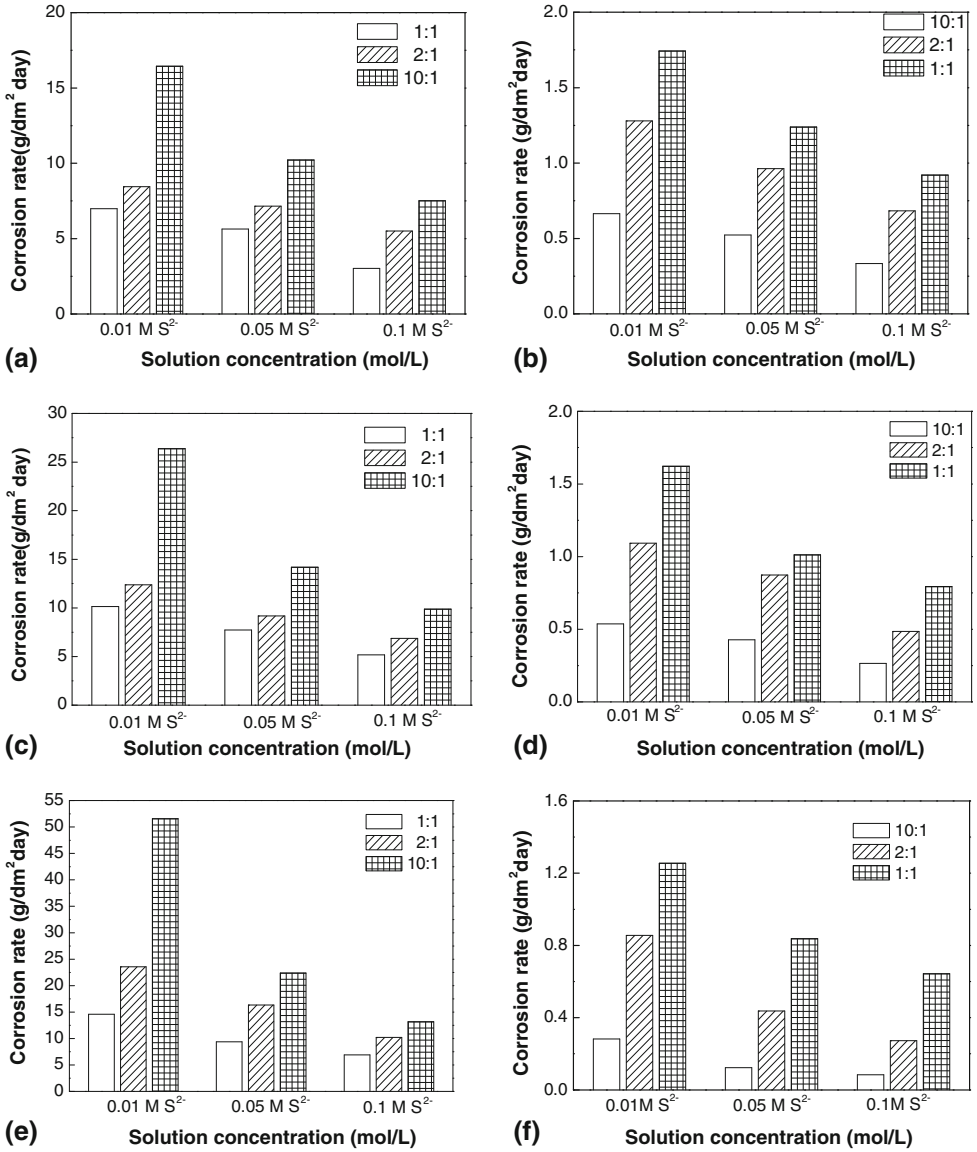

Fig. 3 Corrosion rate of the steels in galvanic couple after various days of immersion in solution (a) 1020 carbon steel, 5 days; (b) 304 L stainless steel, 5 days; (c) 1020 carbon steel, 10 days; (d) 304 L stainless steel, 10 days; (e) 1020 carbon steel, 15 days; (f) 304 L stainless steel, 15 days

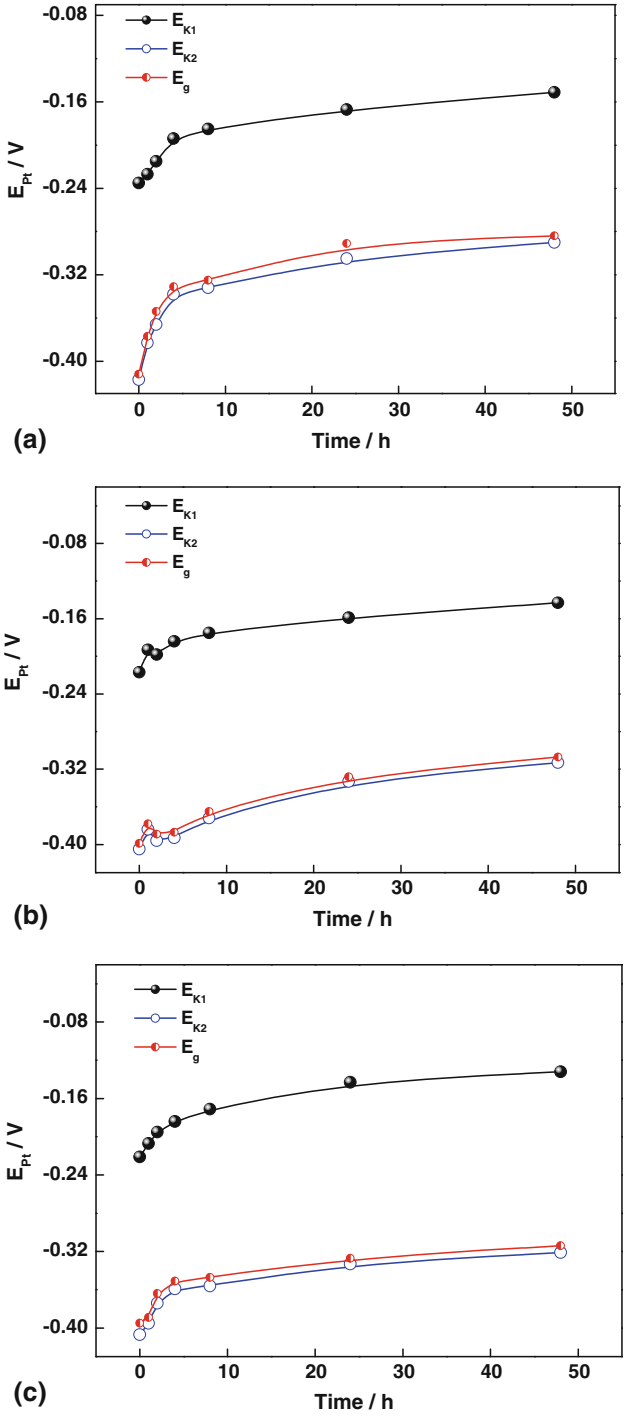

Fig. 4 The corrosion potentials of 1020 carbon steel and 304 L stainless steel and the galvanic potential in 0.10 M NaCl + 0.01 M Na_2S solution with various S_c:S_a ratios (a) S_c:S_a = 1:1; (b) S_c:S_a = 2:1; (c) S_c:S_a = 10:1

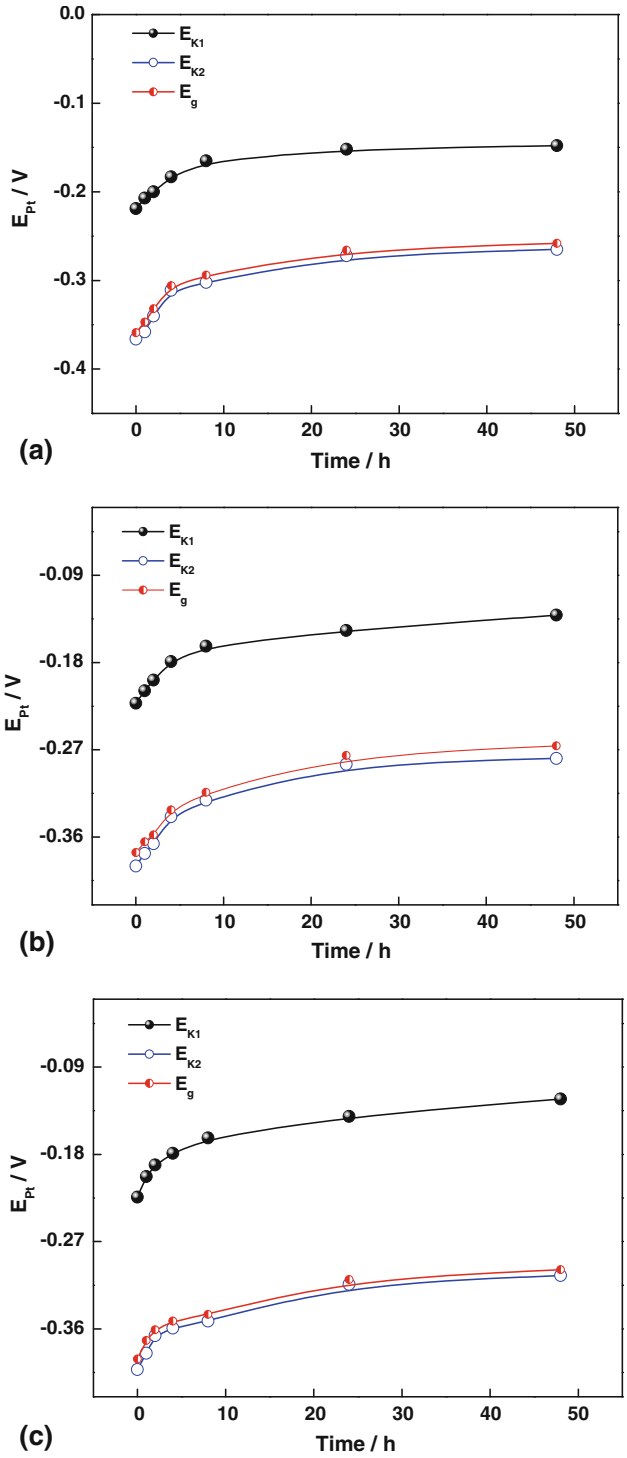

Fig. 5 The corrosion potentials of 1020 carbon steel and 304 L stainless steel and the galvanic potential in 0.10 M NaCl + 0.05 M Na_2S solution with various S_c:S_a ratios (a) S_c:S_a = 1:1; (b) S_c:S_a = 2:1; (c) S_c:S_a = 10:1

with the increasing concentration of S^{2-}. Moreover, with the increase of the cathode/anode area ratio, galvanic current increased significantly.

Figure 3 shows the time dependence of corrosion rate of carbon steel and stainless steel after electrically coupling in the test solutions, where the corrosion rate of individual metal was determined by the weight-loss measurement. The results showed that, at each cathode/anode area ratio, the corrosion rates of carbon steel increased and that of stainless steel decreased with time. Moreover, at individual immersion time, the corrosion rate of carbon steel increased while that of stainless steel decreased with the increasing cathode/anode area ratio.

4. Theory of Galvanic Corrosion

Galvanic effect, γ, is often used to measure the effect of an electrical coupling on corrosion of the couple's metals. Assume that the metal dissolution is the only reaction occurring on anode, galvanic effect can be expressed as (Ref 13, 14):

$$\gamma = \frac{i'_A}{i_A} = \frac{i_g + |i_{Ac}|}{i_A} \approx \frac{i_g}{i_A} \quad \text{(Eq 1)}$$

where i_A and i'_A are the anodic dissolution current density before and after electrical coupling, i_g is galvanic current density, and i_{Ac} is the current density of cathodic reaction occurring on anode.

Galvanic effect can also be determined by the weight-loss measurements as:

$$\gamma = \frac{i'_A}{i_A} = \frac{i_g + |i_{Ac}|}{i_A} = \frac{\Delta W'_A}{\Delta W_A} = \frac{v'_A}{v_A} \quad \text{(Eq 2)}$$

where ΔW_A and $\Delta W'_A$ are weight-loss of the anodic metal before and after electrical coupling, and v_A and v'_A are the corrosion rate of the anode before and after electrical coupling, respectively.

Furthermore, i_g can be replaced by the average galvanic current density during the experimental period (Ref 15), which can be calculated by:

$$i_g = \frac{I_g}{S_A} = \frac{1}{S_A \times T} \int_0^T I_g(t)\,dt \quad \text{(Eq 3)}$$

where S_A is the area of anode exposed to solution, and T is the experimental period. Therefore, the galvanic effect obtained by electrochemical measurements, γ_1, and that determined by immersion tests, γ_2, can be expressed as:

$$\gamma_1 = \frac{i_g}{i_A} = \frac{\frac{1}{S_A \times T}\int_0^T I_g(t)\,dt}{i_{corr}} \quad \text{(Eq 4)}$$

$$\gamma_2 = \frac{\Delta W'_A}{\Delta W_A} = \frac{v'_A}{v_A} \quad \text{(Eq 5)}$$

According to Mansfeld (Ref 13), the relationship between anodic dissolution current density, i_d, galvanic current density, i_g, and galvanic potential, E_g, can be described as:

$$\frac{i_g}{i_d} = 1 - \exp\left\{-\frac{(b_a + b_c)}{0.434 b_a b_c}(E_g - E_{corr})\right\} \quad \text{(Eq 6)}$$

$$i_g = i_d - i_{corr} \exp\left(-\frac{E_g - E_{corr}}{0.434 b_c}\right) \quad \text{(Eq 7)}$$

where b_a and b_c are Tafel slopes of the anodic and cathodic reactions, respectively.

It is realized that the described electrochemical methods applicable for galvanic corrosion research works well for simple corrosion systems. With the complexity of the corrosion process, the actual galvanic corrosion result deviates from the electrochemical prediction, as demonstrated in the following discussion.

5. Discussion

5.1 Galvanic Effect Analysis

The potential shifts, $E_g - E_{corr}$, of both anodic and cathodic materials after electrical coupling in the various solutions are

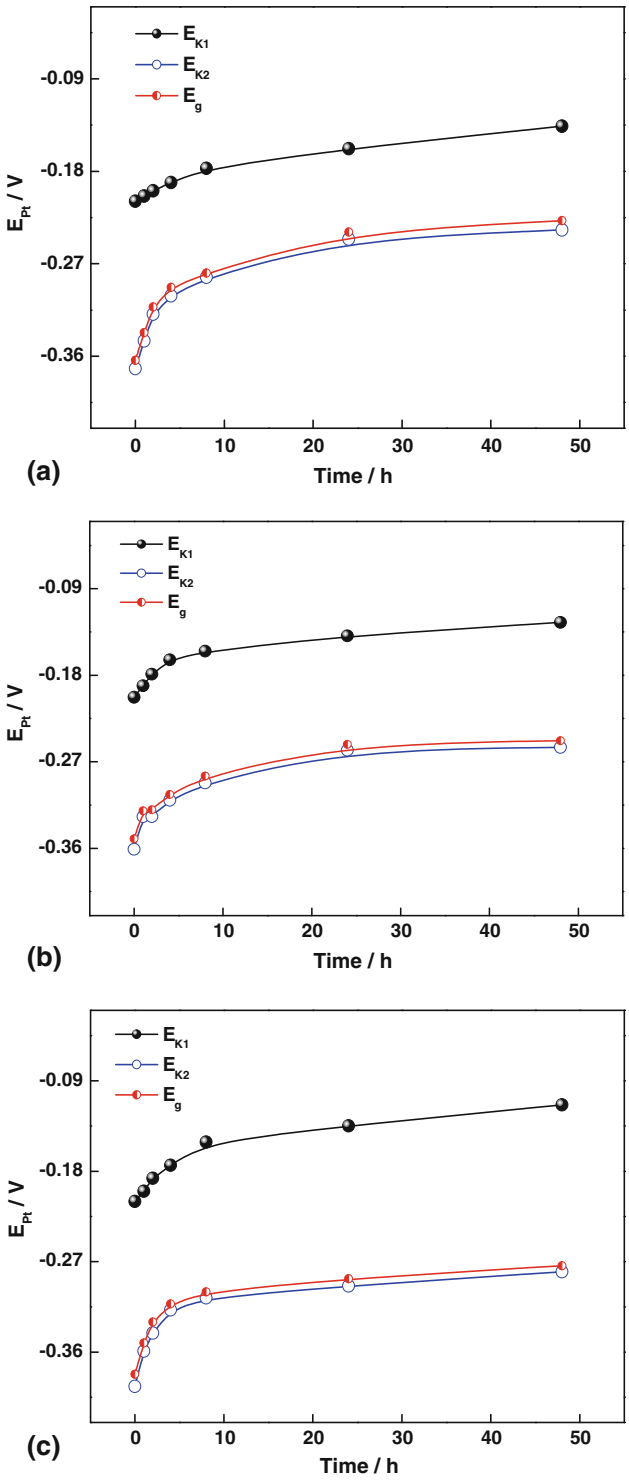

Fig. 6 The corrosion potentials of 1020 carbon steel and 304 L stainless steel and the galvanic potential in 0.10 M NaCl + 0.10 M Na_2S solution with various S_c:S_a ratios (a) S_c:S_a = 1:1; (b) S_c:S_a = 2:1; (c) S_c:S_a = 10:1

Table 3 The galvanic effects of 1020 carbon steel determined by electrochemical measurements and immersion test

Galvanic couple	Solutions	Area ratios	Electrochemical method			Immersion test			
			i_{corr}, A/cm^2	i_g, A/cm^2	γ_1	v'_A	v_A	γ_2	γ_1/γ_2
1020 carbon steel/ 304 L stainless steel	0.10 M NaCl + 0.01 M Na_2S	1:1	1.48	2.31	1.56	10.56	6.73	1.57	0.99
		2:1		2.59	1.75	14.79		2.20	0.80
		10:1		4.74	3.21	31.46		4.67	0.69
	0.10 M NaCl + 0.05 M Na_2S	1:1	1.45	2.03	1.40	7.75	5.52	1.40	1.00
		2:1		2.22	1.53	10.89		1.97	0.77
		10:1		3.04	2.09	15.59		2.82	0.74
	0.10 M NaCl + 0.10 M Na_2S	1:1	1.55	1.73	1.12	5.03	4.31	1.17	0.96
		2:1		2.04	1.31	7.52		1.75	0.75
		10:1		2.40	1.54	10.19		2.36	0.65

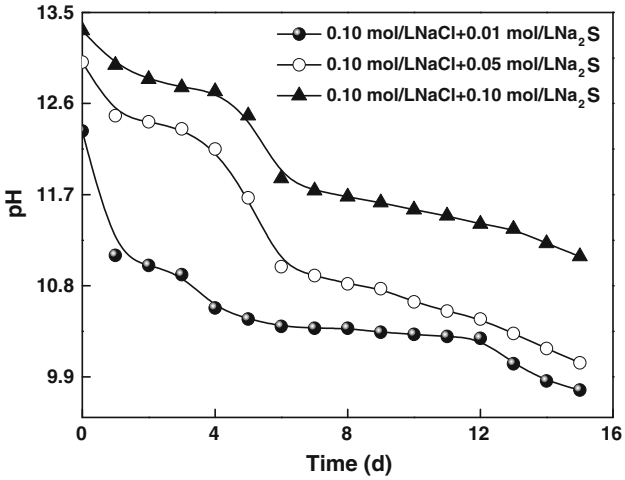

Fig. 7 The solution pH as a function of various S^{2-} concentrations in the solution

shown in Fig. 4 to 6. It is seen that the potential shift of 1020 carbon steel is marginal in all solutions. According to Eq 7, under a small polarization, $E_g - E_{corr} \approx 0$, then $i_g \approx i_d - i_{corr}$. We then have $i_d = i'_A$ and $i_A = i_{corr}$. Equation 1 is thus re-written as:

$$\gamma = \frac{i'_A}{i_A} = \frac{i_g + i_{corr}}{i_{corr}} = 1 + \frac{i_g}{i_{corr}} \quad \text{(Eq 8)}$$

The galvanic effect of 1020 carbon steel determined by both electrochemical method, γ_1, and immersion test, γ_2, as a function of the S^{2-} concentration and cathode/anode area ratio are listed in Table 3. It is seen that, under the individual S^{2-} concentration, both γ_1 and γ_2 increase with the increasing cathode/anode area ratio. The numerical values of both γ_1 and γ_2 are greater than 1, indicating that the electrical coupling enhances corrosion of carbon steel, especially under a big cathode/small anode geometrical arrangement. Moreover, at each cathode/anode area ratio, both γ_1 and γ_2 decrease with the increasing concentration of S^{2-}, indicating the inhibitive effect of S^{2-} on the carbon steel corrosion.

Furthermore, it is shown in Table 3 that the values of γ_1 and γ_2 of the carbon steel are approximately identical ($\gamma_1/\gamma_2 > 0.95$) when the cathode/anode area ratio is 1:1. Thus, the electrochemical measurement and the weight-loss determination give the approximately identical galvanic effect. With the increase of the cathode/anode area ratio, the value of γ_1/γ_2 decreases, indicating that the electrochemical method may not be accurate to determine the galvanic effect. In addition to the dissolution of carbon steel, the cathodic reaction occurring on the surface of anode is not negligible. Therefore, the anodic dissolution current density of carbon steel cannot be replaced simply with the galvanic current density.

5.2 Effects of S^{2-} Concentration on Galvanic Corrosion

This study shows that the galvanic corrosion behavior is affected by the concentration of S^{2-} in the solution, as seen in Fig. 2 and 3. The effect of the S^{2-} concentration on solution pH is shown in Fig. 7. It is shown that the pH value of the solution increases with the S^{2-} concentration. It is acknowledged that the corrosivity of a S^{2-}-containing solution depends strongly on the solution pH. In this study, the pH value of the test solution is around 10, and increases with the S^{2-} concentration. It is anticipated that a layer of iron sulfide will be formed on the carbon steel surface, preventing the anode from further corrosion.

The surface morphology of the electrode after test is shown in Fig. 8. It is apparent that stainless steel is protected from corrosion upon coupling with carbon steel (Fig. 8a). A layer of corrosion product is formed on the carbon steel surface.

The chemical composition of the corrosion products was characterized by EDX, as shown in Fig. 9. The result showed that the atomic mass percent is S:Fe = 35.7495, indicating the potential existence of a compact sulfide film on the steel surface. A further characterization of the film is to be conducted by x-ray photo-electron spectrum (XPS) in the next study.

6. Conclusions

The galvanic effect of the 1020 carbon steel-304 L stainless steel galvanic couple, where carbon steel serves as an anode and stainless steel as a cathode, increases with the cathode/anode area ratio, and decreases with the increasing concentration of S^{2-} in the solution. A layer of sulfide film formed on carbon steel surface to protect it from corrosion.

When the cathode/anode area ratio is 1:1, the electrochemical measurement and the weight-loss determination give the identical galvanic effect. With the increase of the cathode/anode area ratio, the electrochemical method may not be accurate to determine the galvanic effect. In addition to the dissolution of carbon steel, the cathodic reaction occurring on the surface of anode is not negligible. Therefore, the anodic dissolution

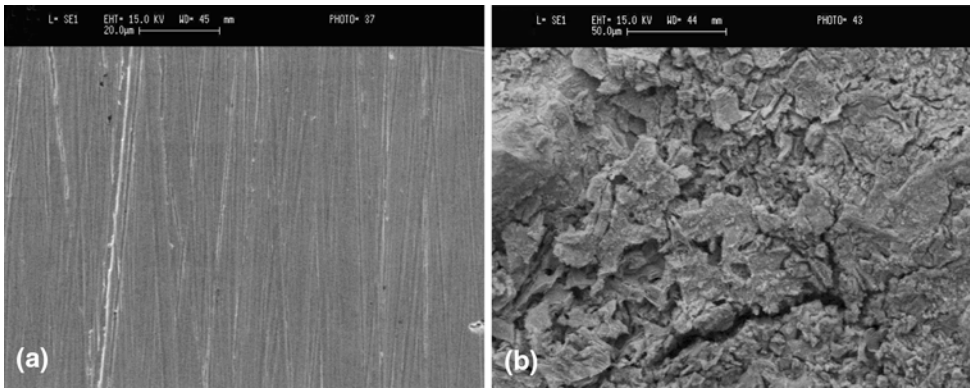

Fig. 8 Surface morphology of specimen after 15 days of immersion in 0.1 mol/l Cl^- + 0.01 mol/l S^{2-} solution (a) 304 L stainless steel, (b) 1020 carbon steel

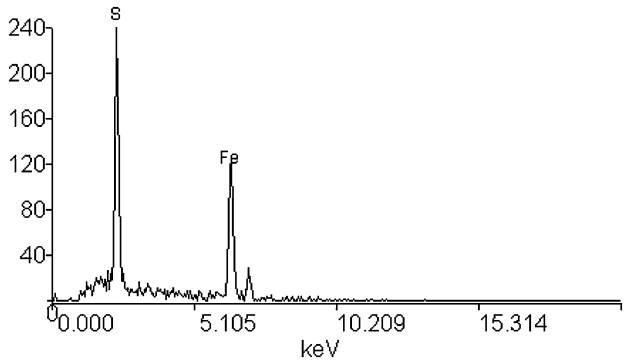

Fig. 9 EDX spectrum of corrosion product formed on the carbon steel surface after immersion test

current density of carbon steel cannot be approximated simply with the galvanic current density.

This study provides an insight into the convenient, reliable evaluation of the galvanic corrosion behavior encountered in industry in terms of the particular galvanic couple geometry.

References

1. J.R. Vera, S. Hernández, C. Scott, and O. Moghissi, *Predicting Galvanic CO_2 Corrosion in Oil and Gas Production Systems, Corrosion/2008*, NACE, Houston, 2008
2. F. Mansfeld, Area Relationships in Galvanic Corrosion, *Corrosion*, 1971, **27**, p 436
3. R. Akid and D.J. Mills, A Comparison Between Conventional Macroscopic and Novel Microscopic Scanning Electrochemical Methods to Evaluate Galvanic Corrosion, *Corros. Sci.*, 2001, **43**, p 1203
4. C.M. Abreu, M.J. Cristobal, and M.F. Montemor, Galvanic Coupling Between Carbon Steel and Austenitic Stainless Steel in Alkaline Media, *Electrochim. Acta*, 2002, **47**, p 2271
5. F.E. Varela, Y. Kurata, and N. Sanada, The Influence of Temperature on the Galvanic Corrosion of a Cast Iron-Stainless Steel Couple (Prediction by Boundary Element Method), *Corros. Sci.*, 1997, **39**, p 775
6. E.P. Rajiv, A. Iyer, and S.K. Seshadri, Corrosion Characteristics of Cobalt-Silicon Nitride Electrocomposites in Various Corrosive Environments, *Mater. Chem. Phys*, 1995, **40**, p 189
7. R.P. Zahran and F.H. Sedahmed, Galvanic Corrosion of Zinc in Turbulently Moving Saline Water Containing Drag Reducing Polymers, *Mater. Lett.*, 1997, **31**, p 29
8. R. Venugopalan and L.C. Lucas, Evaluation of Restorative and Implant Alloys Galvanically Coupled to Titanium, *Dent. Mater.*, 1998, **114**, p 165
9. C. Arya and P.R.W. Vassie, Influence of Cathode-To-Anode Area Ratio and Separation Distance on Galvanic Corrosion Currents of Steel in Concrete Containing Chlorides, *Cement Concr. Res.*, 1995, **25**, p 989
10. D.X. He, T.C. Zhang, and Y.S. Wu, Fretting and Galvanic Corrosion Behaviors and Mechanisms of Co–Cr–Mo and Ti–6Al–4V Alloys, *Wear*, 2002, **249**, p 883
11. ASM, "Corrosion in the Petrochemical Industry," ASM Publication, 1994
12. V.M. Liss, Preventing Corrosion Under Insulation, *US National Board Technical Series Bulletin*, January, 1988
13. F. Mansfeld, The Relationship Between Galvanic Current and Dissolution Rates, *Corrosion*, 1973, **29**, p 403
14. F. Mansfeld, Galvanic Interaction Between Active and Passive Titanium, *Corrosion*, 1973, **29**, p 56
15. F. Bellucci, Galvanic Corrosion Between Nonmetallic Composites and Metals: I. Effects of Metal and of Temperature, *Corrosion*, 1991, **47**, p 808